Preparation and Characterization of Metal-Complex Imprinted PVDF Hollow Fiber Membranes

Xue-Jun Wang,[1,2] Zhen-Liang Xu,[1,2] Nai-Ci Bing,[1] Zuo-Guo Yang[1]

[1]*Membrane Science and Engineering R&D Lab, Chemical Engineering Research Center, East China University of Science and Technology, Shanghai 200237, China*
[2]*State Key Lab of Chemical Engineering, East China University of Science and Technology, Shanghai 200237, China*

Received 24 November 2006; accepted 14 March 2007
DOI 10.1002/app.26805
Published online 20 March 2008 in Wiley InterScience (www.interscience.wiley.com).

ABSTRACT: Using nickel-2,2′-dipyridyl complex as a template, *N*-vinyl-2-pyrrolidone as the metal coordination functional monomer, and ethylene glycol dimethacrylate as the crosslinker, polyvinylidene fluoride (PVDF) hollow fiber ultrafiltration membrane as the supported membrane, metal complex imprinted polymeric membranes were prepared. The association constant of template-monomer interaction in the prepolymerization solution was estimated to be 4.38×10^4 $(L/mol)^2$ by spectrophotometric titration analysis. The attenuated total reflection Fourier transform infrared spectroscopy and scanning electron micrograph characterization indicated that the surface of the support PVDF membrane was completely coated by the imprinted polymer layer after modification. The imprinted membranes exhibited the selective permeability for the template in certain nickel acetate solution. The molecularly imprinted membranes gave higher permeation separation factors at about pH 6, whereas increasing pressure would lower the separation ability. The effects of ion concentration, cations and counterions, ligand selectivity, pH, and trans-membrane pressure were investigated and the permeation performances of the imprinted membranes could be regarded as facilitated transport mechanism. © 2008 Wiley Periodicals, Inc. J Appl Polym Sci 109: 64–73, 2008

Key words: molecular imprinting; molecularly imprinted membrane; metal–complex; polyvinylidene fluoride

INTRODUCTION

Interest in membranes has been increasing in various fields of science and technology because of the recognition that membranes play an indispensable role for the solving of basic problems confronted by the present world, such as resource, energy, information, environment, artificial organs, and so on. Membrane separation has attracted much attention owing to its promising properties such as easy and low energy of continuous operation under mild conditions, better feasibility to sale-up, and the resulting low cost of operation.[1] The selectivity of membranes for a targeted molecule is a key factor determining the success of a membrane separation process. Many efforts have been made to prepare membranes having selectivity towards specific molecules,[2] in which, molecular imprinting is the most applicable method for the construction of polymeric materials for molecular recognition.[3,4]

Two different approaches have been developed to produce molecularly imprinted polymers (MIP): the set up of covalent interactions between template molecules and monomers[5,6] and the development of reversible noncovalent interactions between them.[7,8] Traditional applications of MIP in the sensing and separation utilize polymer particles obtained by grinding and sieving of synthesized block-polymers,[9,10] suspension,[10–12] or precipitation[13,14] polymerizations. However, new MIP formats are being developed to avoid the limitations of the traditional approach—first of all long preparation times, mechanical deformation of the binding sites during grinding of bulk polymers, time-consuming sieving procedure necessary for the isolation of the fraction with a narrow size distribution associated with high material loses. Generally, the use of small polymer particles in the separation process is often associated with the generation of too high backpressures. Development of highly porous supported or free-standing imprinted membranes would solve most of these problems.

Molecularly imprinted membrane (MIM) offers the advantage to combine the mechanical integrity of the support membrane and the selectivity of the imprinted polymer. The application of MIP to membrane separation was first reported by Piletsky et al.[15] After that various methods were reported to prepare MIM, which can be summarized as follows: dry or wet phase separation,[16,17] surface imprint-

Correspondence to: Z.-L. Xu (chemxuzl@ecust.edu.cn).
Contract grant sponsor: National Fund; contract grant number: 2003CB615705.

ing,[18,19] *in situ* polymerization,[20] and molecularly imprinted nanospheres or particles composite membrane.[21,22] However, the fluxes of membranes made from immersion precipitation phase inversion or bulk polymerization are rather low.[23,24] Moreover, it is difficult to prepare thin and stable membranes with the reproducible properties from highly cross-linked polymers. In contrast, membrane modification by *in situ* polymerization on the surface of the already flux-optimized microfiltration (MF) or ultrafiltration (UF) membranes in the presence of a template has been shown to be a feasible novel approach.[25–27] In all these recognition systems, the hydrogen and electrostatic interactions between monomer and template were widely used, while the metal coordination was less studied. Metal-coordination interactions have structural and catalytic roles in nature, and have been exploited in the development of molecular recognition systems[28–31] with the virtue of stronger interaction than hydrogen bonds and van der Waals forces, higher stability in the polar aqueous-alcohol system and easier preorganization than with other interactions. To date, there are only few reports[32–34] on the preparation of MIM using metal coordination as the interaction between monomers and polymers. Usually, the imprinted layer was coated on a flat sheet membrane and the permeation performance was evaluated under quiescent conditions or by stirring the solutions.

In the present work, the surface imprinting technique was employed to prepare the metal-complex selective permeation composite membranes. To obtain flexible and mechanically stable membranes for practical application, porous polyvinylidene fluoride (PVDF) hollow fiber UF membrane was used as support. The morphology of the imprinted membrane was characterized by scanning electron microscopy (SEM). To evaluate selectivity and imprinting effect for the metal complex, the permeation experiment was carried out under dynamic conditions, and the effects of pH and different ions on the permeation process were also investigated. Finally, the origin of selective permeation and the mechanism of metal complex transport through the membrane were discussed.

EXPERIMENTAL

Reagents and materials

N-vinyl-2-pyrrolidone (NVP) was obtained from Fluka (Buchs, Switzerland). Ethylene glycol dimethacrylate (EDMA) was obtained from Shanghai Coral Chemical Co. (Shanghai, China). 2,2′-Azobisisobutyronitrile (AIBN) and 2,2′-dipyridyl (dipy) were obtained from Sinopharm Chemical Reagent Co. (Shanghai, China). Methanol, acetic acid, nickel acetate, and other chemicals were of analytical grade. EDMA and NVP were distilled to remove the inhibitors and AIBN was recrystallized with ethanol before use. The pH value of the solutions was adjusted with hydrochloric acid for pH 2–6 detected using PHS-3C digital pH meter (Shanghai Precision & Scientific Instruments Co., China). PVDF hollow fiber UF membranes were spun using phase-inversion method,[35] and the molecular weight cut-off of the membranes is ~10,000.

Preparation of metal complex imprinted membranes

To produce the imprinted polymer layer of MIM1, PVDF hollow fiber membranes were coated by soaking in a 10-mL methanol solution containing 156 mg dipy (1.0 mmol) and 249 mg Ni(II) acetate (1.0 mmol), 2.0 mmol NVP, 20 mmol EDMA, and 40 mg AIBN. After that, membranes were placed in an oven and sparged with N_2 for 5 min. Here, the solvent methanol also serves as the porogen to create pores in macroporous polymers.[36] Then, the oven was sealed under vacuum and the polymerization was initiated thermally at 65°C and continued for 24 h. The membranes were then extracted with methanol/acetic acid (7/3, v/v) overnight and washed with distilled water to remove any nongrafted polymer, monomer, residual initiator, and the template. The efficiency of this procedure was checked by the filtration of distilled water through selected samples and recording of the UV spectrum of the filtrate. The absorbance was <0.005 at 310 nm. The extracted membrane was then dried to constant weight under vacuum at 60°C and the degree of coating was calculated from the difference in weight between the modified membrane with deposited MIP layer and the initial membrane.

Two reference membrane systems were similarly prepared: MIM0 without Ni(II) acetate and NIM without Ni(II) acetate and dipy during the polymerization.

Spectrophotometric analysis of template-monomer interaction

An UV762 spectrophotometer (Shanghai Precision & Scientific Instruments Co.) was used to determine the content of metal-complex. A series of solutions were prepared with a fixed concentration of equivalent NVP and metal ion (0.02 mmol/L) and various amounts of dipy in methanol. The absorption spectra of these solutions with corresponding dipy solutions as references were determined at 228 nm.

Characterization of the composite membranes

The surface structures of the support and imprinted membranes were analyzed by attenuated total reflection Fourier transform infrared spectroscopy (ATR-

FTIR) on a Nicolet 380 FTIR instrument (Thermo Electron, USA).

The morphology of the support membrane and imprinted composite membrane was examined by SEM using a JEOL model JSM-6360 LV (Japan) scanning electron microscope. The surface and cross-section of hollow fiber membranes were sputtered with gold after breaking the membranes in liquid nitrogen to avoid destroying the structure of the cross sections and observed at a voltage of 15 kV.

Measurement of coating degree, water content, and swelling ratio of the membrane

The coating degree (D_c) was defined as follows:

$$D_c = (m_c - m_o)/m_o \quad (1)$$

where m_o and m_c are the weight of original and coated membrane.

The water content of the membrane was calculated by use of the equation:

$$W_c(\%) = \frac{m_{\text{wet}} - m_{\text{dry}}}{m_{\text{dry}}} \times 100\% \quad (2)$$

where m_{dry} and m_{wet} are the weight of dry and wet membrane.

The wet membrane was prepared by immersing the dry membrane in deionized water for 24 h at room temperature, centrifugation at 3000 rpm for 2 min and weighing. And the swelling ratio (R_w) of the membrane was calculated as follows:

$$R_w = V_{\text{wet}}/V_{\text{dry}} \times 100\% \quad (3)$$

where V_{dry} and V_{wet} are the volumes of the dry and the wet membrane, respectively. The volumes of the dry and the wet membrane were calculated from the length and the inner and outer diameter of the hollow fiber membranes in the dry and the wet state, measured with a ruler or micrometer.

Binding experiments of dipy on MIM with the mediation of metal ions

In 50 mL polyethylene bottles, the metal ion aqueous solution was added with equivalent dipy and immersed MIM1 with shaking at 25°C for 12 h. Membrane syringe filter (Shanghai Institute of Pharmaceutical Industry, China) was used to clarify the solutions for further analysis. The concentration of $[\text{Ni-dipy}]^{2+}$ was determined with UV spectrum at 310 nm and the binding capacity Q (μmol/g) of dipy on membrane could be calculated as follows:

$$Q = V(c_0 - c)/m \quad (4)$$

where V, c_0, and c represent the volume, the initial and equilibrium concentrations of the solution, respectively, and m the mass of polymer sample.

Permeation flux of pure water and analytes through the membranes

Four hollow fibers were selected and cut into a length of 25 cm and potted at both ends with epoxy glue in a test module. The membrane module, with an effective surface area of about 25 cm^2 based on the average of outer diameter, was mounted on the membrane separation apparatus (Fig. 1). The feeding was with an aqueous solution with a concentration of 20 μmol/L $[\text{Ni-dipy}]^{2+}$ if no other notes. The amounts of the $[\text{Ni-dipy}]^{2+}$ that permeated through the membrane were determined by analyzing an aliquot of the solution from the receiving phase with the UV spectrophotometer. In all the permeation experiment, the module was filtrated using pure water for 1 h, and then the feed solution was used to filtrate in a total-reflux mode before measuring the permeation data, which we think can guarantee the steady state fluxes. Three modules for each kind of membrane (imprinted or not) were used to permeation tests. Each module was determined for three times, and the average was obtained as result. All permeation experiments were carried out at room temperature and 1 Bar if no other notes.

The pure water flux F_p (L/m^2 h Bar) and total permeation flux J (μmol/m^2 h Bar) of the membrane is obtained as follows:

$$F_p = \frac{V}{At\Delta P} \quad (5)$$

$$J = \frac{Vc}{At\Delta P} \quad (6)$$

where V is the total volume of permeate, c is the concentration of the permeate, A is the effective sur-

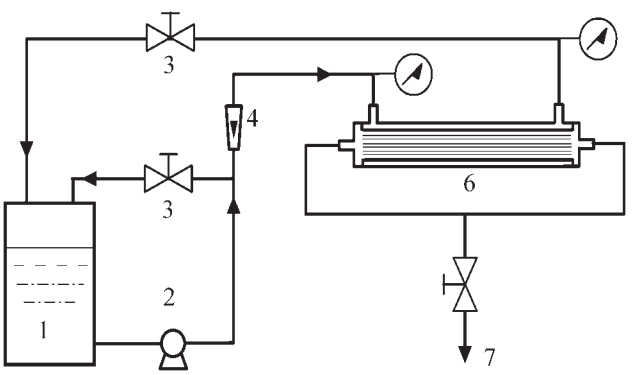

Figure 1 Schematic illustration of membrane separation system. 1, Tank; 2, pump; 3, valve; 4, flow meter; 5, pressure gauge; 6, membrane module; 7, permeate.

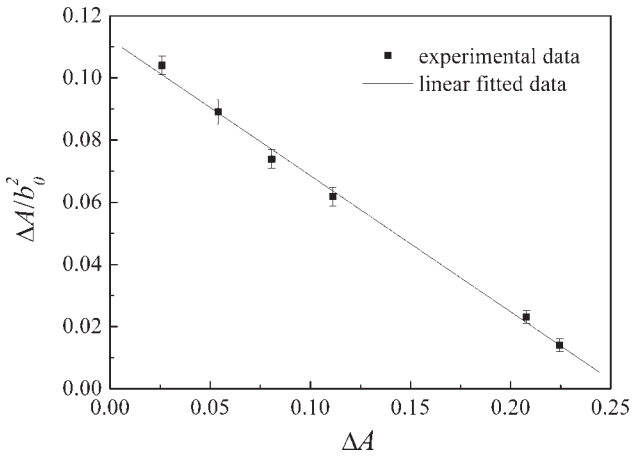

Figure 2 Plot of $\Delta A/b_0^2$ versus ΔA at 228 nm. Plots obtained from the titration of 0.02 mmol/L $[Ni\text{-}dipy]^{2+}$ against monomer in concentration range of 5–40 mmol/L.

face area of the membrane composed in one module, t is the running time, and ΔP is the operation pressure. The effective filtration area of hollow fibers is calculated upon the outer diameter of the fibers.

The separation factor (α) of 2,2′-dipy(A) towards 4,4′-dimethyl-2,2′-dipy(B) can be defined as follows:

$$\alpha = \frac{c_{p_A}/c_{f_A}}{c_{p_B}/c_{f_B}} \tag{7}$$

where c_{fA}, c_{fB}, c_{pA} and c_{pB} are concentrations of A and B in the feed and permeation solutions, respectively. The background solution pH was adjusted using 0.1*M* HCl solution. Nickel hydroxide precipitation occurs above pH 6.5, which also depends on the concentration of nickel in the medium. In consideration of hydrolysis, pH above 6 was not tested.

RESULTS AND DISCUSSION

UV characteristics of the prepolymerization solution

The strength and positioning of the monomer-template interactions are crucial to obtain polymers with good molecular recognition properties. Evaluation of the binding interactions between a template and a functional monomer is one of the key steps during the design of MIP. Since we are interested in the development of $[Ni\text{-}dipy]^{2+}$ imprinted functional materials as separation membrane, we have evaluated the binding interactions of $[Ni\text{-}dipy]^{2+}$ with NVP using spectroscopic method[37,38]:

$$\Delta A/b_0^n = -K\Delta A + K\Delta\varepsilon a_0 l \tag{8}$$

where n is the composition of the complex; ΔA is the absorbance difference between the mixture of $[Ni\text{-}dipy]^{2+}$ with NVP and corresponding dipy solutions when $b_0 >> a_0$(the equilibrium concentration of B and A); $\Delta\varepsilon$ is the difference of molar absorptivities between complex C and template A; and K refers to the association constant between template A and monomer B in the reaction (9):

$$\mathrm{A} + n\mathrm{B} \xrightarrow{K} \mathrm{C} \tag{9}$$

Now K and n can be obtained by plotting $\Delta A/b_0^n$ versus ΔA.

The appropriate plots of $\Delta A/b_0^n$ versus ΔA according to eq. (8) give straight lines whose slopes give K. In present work, the plot of $\Delta A/b_0^n$ versus ΔA is linearly regressed to get $n \approx 2$ and K is calculated to be 4.38×10^4 $(L/mol)^2$, from its slop (Fig. 2). This indicates the 1 : 2 complexes of templates and the monomers may be predominating in the prepolymerization mixture and the interaction is stronger and more stable than that of complexes formed with hydrogen bonds.[38] On the basis of this, we put forward the possible binding mode in the course of prepolymerization and polymerization (Fig. 3).

ATR-FTIR of the composite membranes surfaces

Figure 4 shows the ATR-FTIR spectra of (a) support membrane and (b) extracted imprinted composite membrane. It can be seen that the shape and position of all peaks in both IR spectra are exhibited in a different way. Figure 4(A) is the surface ATR IR spectra of support membrane. The absorption peaks of 1404, 1043, 880, and 840 cm^{-1} are the typical

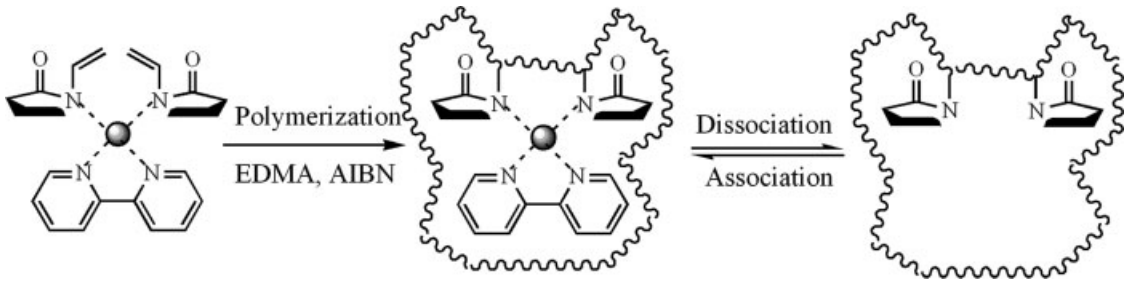

Figure 3 Schematic representation of the imprinting process.

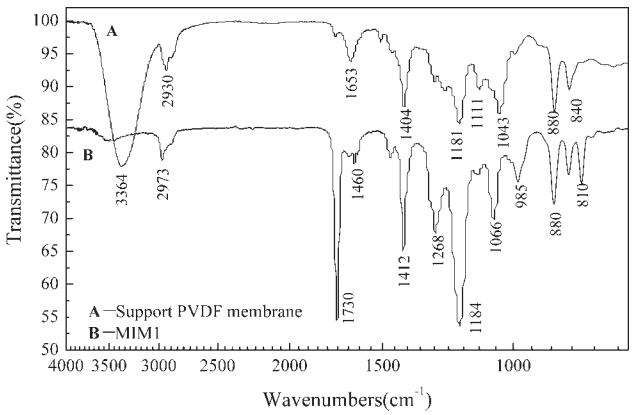

Figure 4 ATR-FTIR spectra of imprinted membrane and support membrane. A. Support PVDF membrane. B. Imprinted membrane (MIM1).

absorption peaks of PVDF. The peak at 2930 cm^{-1} corresponds to dissymmetry stretching vibration of $—CH_2—$, and there are no obvious absorption bands between 2960 and 2950 cm^{-1}, which indicates no $—CH_3$ in the PVDF polymer.

In the infrared spectra of Figure 4(B), the strong absorption peak 1730 cm^{-1} should correspond to absorption bands of —C=O stretching vibration. And the features around 1066 cm^{-1} and 1184 cm^{-1} indicate the symmetric and dissymmetry stretching vibration of —C—O—C of ester, respectively. The peak at 2973 cm^{-1} is assignable to absorption bands of $—CH_2—$ or $—CH_3$ stretching vibration and another absorption peak near 1458 cm^{-1} should contribute to the bend vibration of $—CH_3$ or forficiform vibration of $—CH_2—$. No obvious bands were present in the region 1648–1638 cm^{-1} indicating the absence of vinyl groups in imprinted polymeric surface layer, which suggests that both NVP and EDMA are polymerized.

It is concluded that the surface of the support PVDF membrane has been completely coated by the imprinted polymer layer, which leads to the disappearance of typical peaks of PVDF and the emergence of the typical peaks of imprinted polymer.

Morphology of the composite membranes

Membrane morphology was examined by a SEM. In Figure 5, It is evident form the cross-sectional images [Fig. 5(C,E)] that the support PVDF membrane has an asymmetric structure, which consists of a thin and dense outer layer, and a thick porous layer with sponge-like structure pores less than 1 μm. The surface micrographs show that the outer surface of the PVDF support membranes [Fig. 5(A)] is completely covered by a thin layer [Fig. 5(B)] after the modification procedure. The modified membrane's surface seems smooth and flexible. The formation of a very thin imprinted polymer layer can also be found in the cross-section of the imprinted membrane, as shown in Figure 5(D,F).

Pure water flux and binding capacity

For all the figures given in the Table I, the standard deviations are less than 5%. As shown in Table I, the coating degrees of the two nonimprinted membranes MIM0 and NIM are higher than the imprinted one MIM1. The slight difference may come from the washing procedure. And more likely, it can be attributed to the existence of Ni^{2+} that influences the polymerization of imprinted layer. MIM1 showed better binding performance than other two membranes, due to the recognition cavities formed in the MIM1 imprinted layer. Pure water flux measurements (at 2.0 Bar and 25°C) of the original and modified membranes (with and without template) showed that the modification process caused a decrease in membrane permeability (F_p). The decrease is more pronounced in the case of the nonimprinted membrane than the imprinted membranes. The pure water fluxes of three modified membranes are also lower than those before template removal, which is only about 9.2 $\pm$ 0.5 L/m^2 h Bar. This is because of the formation of cavities after removal of the template molecule from the imprinted layer. At the same time, the pores and channels in the imprinted layer may be connected, which would also increase the flux. The water content of the three coated membrane are close and all higher than blank PVDF hollow fiber support membrane, which is the result of hydrophilization of surface after coating polymerization. At the same time, the highly cross-linked coating layer made the membrane has lower swelling ratios.

Ion concentration on permeation performances

Transport studies with MIP membranes can provide a deeper understanding of the relationship between the shape of the template cavities and the arrangement of the functional groups of functional monomer in these cavities. The dependence of dipy permeation on Ni(II) acetate concentration was examined for each of the membrane systems using 20 μmol L^{-1} dipy solutions mediated with varied concentrations of Ni^{2+} (Fig. 6). The concentration of Ni^{2+} had a remarkable effect on the permeation performance of dipy through MIM1, which suggests that the Ni^{2+} plays an bridge-like role in the recognition process and the binding target should be $[Ni\text{-}dipy]^{2+}$ with coordination interaction. Optimum transportation of dipy through MIM1 was achieved at a 1 : 1 mole ratio of Ni^{2+} to dipy as expected. The presence of Ni^{2+} was therefore a necessary requirement for selective recognition of dipy, with greatly

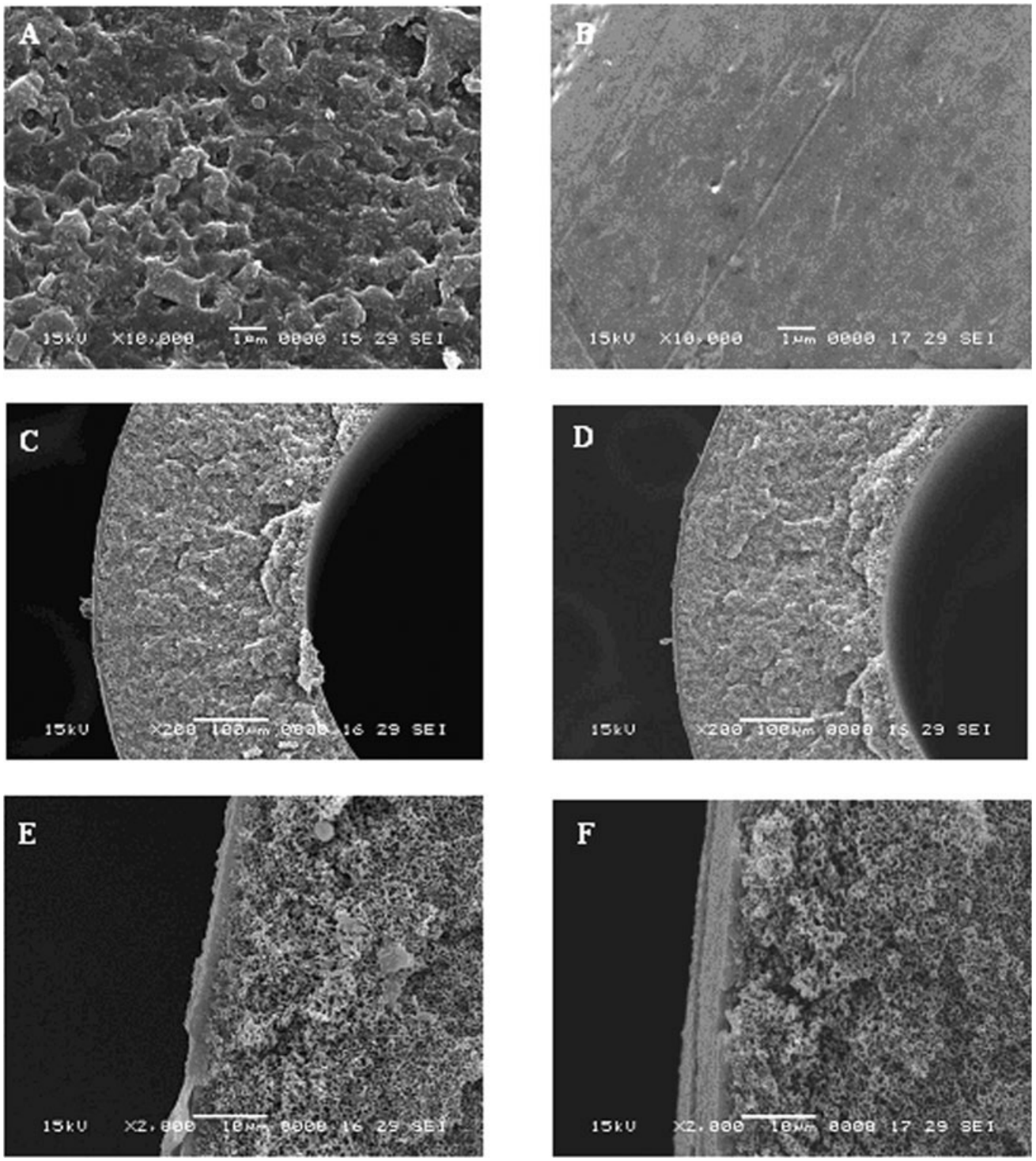

Figure 5 SEM images of the PVDF membrane (A, C, E) and imprinted composite membrane (B, D, F); A and B: external surface of the membranes; C, D, E, and F: cross-sections of the membranes.

decreased permeation rate observed in its absence. The decrease in permeation rate after this point indicates that the excess Ni^{2+} in the solution competes more successfully on MIM1 than the analyte [Ni-dipy]$^{2+}$. It should be noted that at a 1 : 2 mole ratio of Ni^{2+} to dipy, the permeation rate of all three membrane systems were all decreased. That could be due to the formation of [dipy-Ni-dipy]$^{2+}$ complex, which increased the transport resistance.

Ligand selectivity of membrane transportation

The permeation properties were investigated using a feeding solution with concentration of 20 μmol/L

TABLE I
Characterization of Imprinted and Nonimprinted Membranes

Membrane	Coating degree D_c (%)	Binding capacity Q (μmol/g)	Pure water flux F_p (L/m^2 h Bar)	W_c (%)	R_w (%)
Blank PVDF	–	–	81.04	35.7	1.15
MIM1	0.88	0.465	13.53	46.1	1.10
MIM0	0.91	0.206	12.44	45.9	1.09
NIM	0.97	0.093	10.14	42.8	1.07

[Ni-ligand]$^{2+}$. As shown in Figure 7, the metal-complex imprinted membrane has larger permeation flux than the other two membranes. The different transport results of imprinted and nonimprinted membrane can be inherited from different polymer morphology between polymerization with or without template molecule. The presence of template molecule during polymerization makes the membrane to have different structure, porosity, and swelling. The different sizes of micropores in imprinted and nonimprinted membrane may lead to differences in transport of analyte of different molecular size.

The transport properties of imprinted polymer membrane were investigated using several ligands, including 2,2′-dipy, 4,4′-dipy, 4,4′-dimethyl-2,2′-dipy, and 1,10-phen. Figure 7 shows the good selectivity for the different ligands across the imprinted polymeric membrane (MIM1), while the transport rates of all the analytes across the nonimprint membrane differs only slightly and are slower compared with those of the imprinted polymer membrane. MIM1 demonstrated higher permeation rate for 4,4′-dipy than for dipy, mainly because 4,4′-dipy is hard to coordinate Ni^{2+} with bident and can transfer through the micropores in MIM1 without to much hindrance. The lower permeation rate of the bulkier ligand 4,4′-dimethyl-2,2′-dipy was indicative of lower affinities for Ni^{2+} centers in the polymer. At the same time, this suggests steric factors limit its accessibility to the sites and paths generated using the smaller ligand, dipy. The similar permeation rate of 1,10-phen with dipy illustrates the shape selectivity of the molecularly imprinted recognition sites. For 2,2′-dipy imprinted MIM0, there were no effective and strong interactions between 2,2′-dipy and NVP in the phase of preorganization without Ni^{2+}. Even though some amorphous pores or cavities were formed with the existing porogens, MIM0 showed no imprinting effect or selectivity.

As to the selective transport of the molecular imprinted membrane, besides sieving, two different mechanisms should be regarded[4]: (1) Facilitated transport: the nonspecific analysts (nontemplate) did not transport or its rate of transport was slower because of the preferential sorption of the template together with the better transport path matched with size and shape of the template. (2) Retarded transport: the permeation of the template molecules was retarded owing to affinity binding (the interaction between the functional groups in cavities and the template was relatively strong than the nontemplate molecules). In this case, the transport rate of the target molecules and its structural analogue depends on the former mechanism that has dominant effect, which will be further confirmed by the following results.

Effect of cation and anion on permeation

The influence of ions on the permeation performances of membranes was also studied with $Co(Ac)_2$,

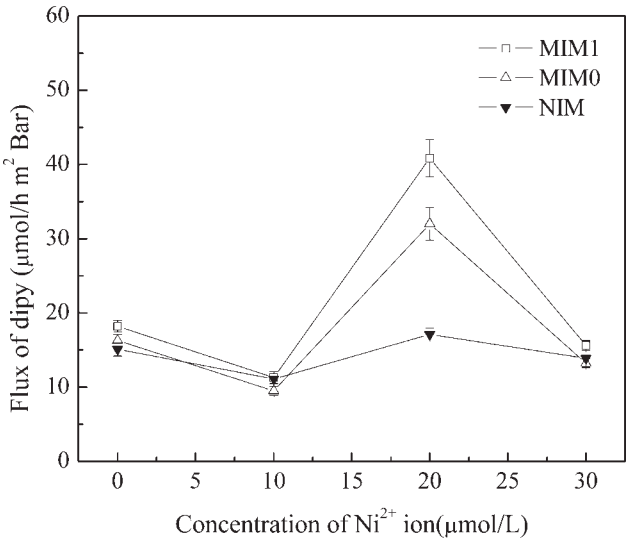

Figure 6 Effect of ion concentration on membrane permeation performances.

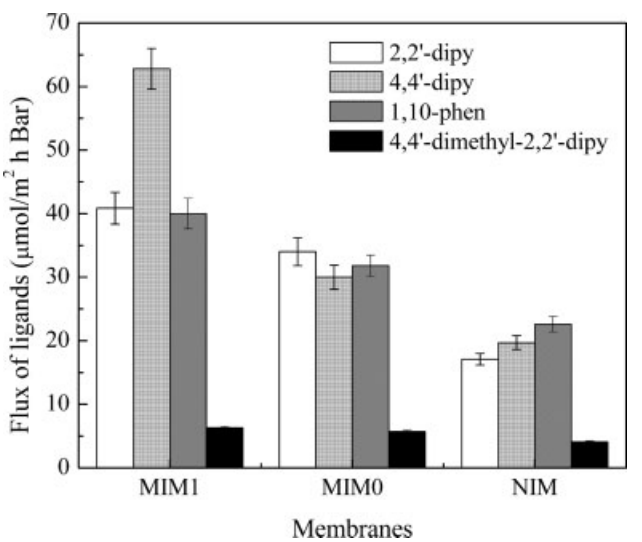

Figure 7 Ligand selectivity of imprinted and nonimprinted membranes.

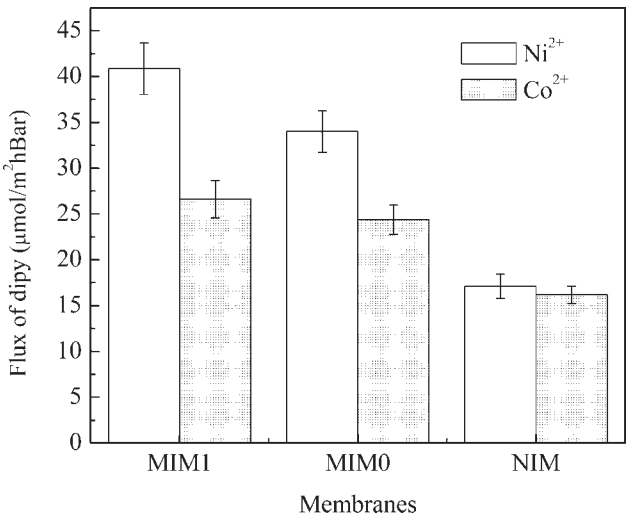

Figure 8 Effect of cations on membrane permeation performance.

$Ni(Ac)_2$ for cation system, and $Ni(NO_3)_2$, $NiCl_2$, and $Ni(Ac)_2$ for anion system.

The substitution of Co acetate for Ni acetate in the solution was performed to examine the effect of cation on permeation. Figure 8 revealed superior ligand selectivity in the case of Ni^{2+} acetate. The observed permeation rate of dipy was higher for MIM1 than those for the reference membrane systems. Both ions posses similar ionic radii, $r_{Ni(II)} = 0.070$ nm, $r_{Co(II)} = 0.072$ nm, suggesting that amongst this group ionic bulk should not be a controlling factor. However, preferred coordination geometries between two species are quite distinct, as only Ni^{2+} shows a preference towards tetrahedral complex formation, while Co^{2+} tends to be octahedral. So the cavity on the polymer suitable for Ni^{2+} complex was not suitable for the other complexes. Matsui et al.[29] has reported strong nonspecific Ni^{2+}-mediated binding of dibenzoylmethane on Co^{2+} imprinted polymer, which we suggest may arise from the same reason. The effect of different metal ions revealed that this recognition process is not only targeted on the metal–dipy complex but also controlled by the special structure and spatially arranged functional groups of MIP, which is the result of molecular imprinting.[30]

The effect of the Ni^{2+} counterion on ligand permeation rate by MIM1 was examined by substitution of nickel chloride and nitrate for nickel acetate. The permeation rates of dipy were 40.85, 34.62, and 31.27 μmol/m^2 h Bar for nickel chloride, nitrate, and acetate, respectively. Comparison of permeation rate across MIM1 revealed no effective recognition in the presence of these alternate counterions. It is proposed that the relative strength of cation–anion associations gives rise to this effect,[29] i.e., Ni^{2+}-acetate is weaker than Ni^{2+}-polymer, which in turn is weaker than Ni^{2+}-chloride and nitrate. Wu et al.[31] has suggested that the anion had participated in recognition process. When anion had been changed, the size and even the shape of complex may be changed because of the differences of the anions and their binding to metal ions, which led to the lost of molecular imprinting effect.

Effect of pH on permeation

Since the interaction between the MIPs and the tested analyte depends on metal coordination association, the effect of pH of the feeding solution on MIM1 permeation performances and selectivity was investigated along with that of the nonimprinted and the control membranes.

Permeation performances of imprinted and nonimprinted membranes were influenced by the pH of the feed solution (Fig. 9). With a decreasing pH, the permeation rate was enhanced for both MIM1 and MIM0. This behavior suggests that complexation between the metal ion and amide groups immobilized on the polymer matrix plays a substantial role in the recognition of the metal ions. It is easy to find that the pH influence the permeation rate of MIM1 more remarkably than that of MIM0 and NIM. This result can be attributed to the imprinting effect: by template imprinting technique, selectivity cavity or binding sites would be effectively created on the accessible internal surfaces of MIM1. The selective transportation of different ligands may arise from the specific recognition and mass transfer mode of imprinted membrane. First, the proper ligand binds on the recognition sites of the imprinted membrane. And then the coordination forces in metal-complex are damaged soon after they are formed. Thus, the ligand moves or diffuses to the deeper side of the

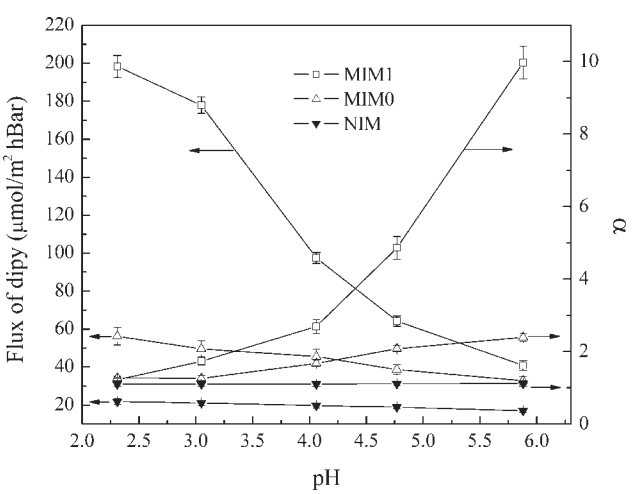

Figure 9 Effect of pH on membrane permeation performances and separation factors.

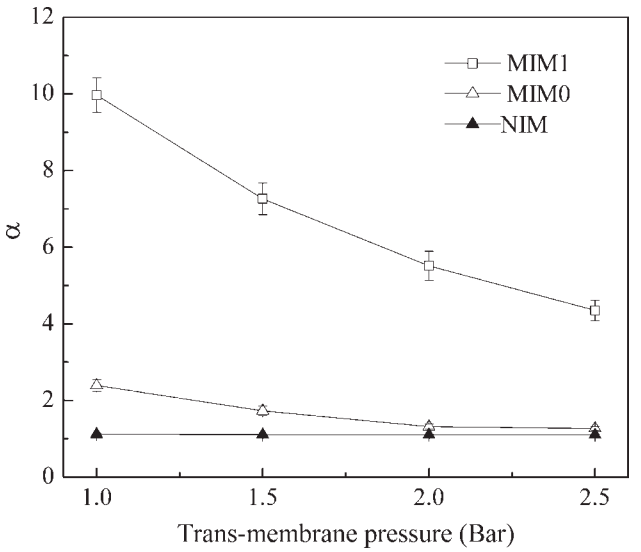

Figure 10 Effect of pressure on membrane separation factor.

membrane with the destruction of the ion-amino group under certain pH values. Step by step, the selective sorption of the template together with the better transport path matched with size and shape of the template lead to the preferential permeation of the ligand through the imprinted membrane.

The separation factors (α) of 2,2′-dipy(A) towards 4,4′-dimethyl-2,2′-dipy decreased with the decreasing of pH. When pH = 2.31, $\alpha \approx 1$, which means no selectivity was showed at that point. In the investigated pH range, the highest α was given at about pH 6. This can be explained that the complex of $[Ni\text{-}dipy]^{2+}$ is stable in the neutral system, which could give the optimum selectivity. While when the pH decreased, the complex $[Ni\text{-}2,2'\text{-}dipy]^{2+}$ was protonized and degraded, which led to lower or even no selectivity.

Effect of operation pressure on permeation

The separation rate and the efficiency of traditional UF process could be adjusted by changing the operation pressures. In this work, the effect of operation pressure on the separation factor of the membranes was investigated under different operation pressures with fixed feed concentration of $[Ni\text{-}dipy]^{2+}$. As seen in Figure 10, the separation factor of the imprinted membrane MIM1 decreased obviously with the increasing of operation pressure, although the macroscopically driving force of the permeation increased with the increasing operation pressure. This is because the microstructures of imprinted layer and the support bulk membrane maybe were pressed and distorted, which would reduce or close the channels or paths and block the molecules to pass. At the same time, the recognition and separation ability of the recognition sites and cavities are negatively affected by the increasing operation pressure and the transferring rate of the analytes was relatively lowered subsequently, which caused the separation factor decreased. While for the other two membrane systems, especially the MIM0, the changes of pressure resulted in no obvious differences to their separation factors, which means they showed little or no imprinting effect.

CONCLUSIONS

Membranes with a thin layer of imprinted polymer using water-soluble metal-complex as template were developed and permeation properties of these membranes were studied. The association constant of template–monomer interaction in the prepolymerization solution was estimated to be 4.38×10^4 $(L/mol)^2$ by spectrophotometric titration analysis. The ATR-FTIR characterization and SEM images of imprinted membrane indicates that the PVDF support membrane was completely covered by a thin layer. The ability of the new MIP hollow fiber membranes was capable of selective permeation of its original imprinting template. This was, probably, a result of both multisites binding to the template via metal coordination and the correct position of functional groups involved in binding in imprinted polymeric membrane. The influencing factors that affect the membrane permeation performances were investigated, including ion concentration, cations and counterions, ligand selectivity, pH, and pressure. The results showed that it is possible to adjust the permeation performance of MIP membranes by varying of pH values, which could be used in the controlled drug release system. The method proposed here can also be looked as a solution to the imprinting problem of small molecules and molecular recognition in strong polar solvent such as aqueous medium.[39,40]

References

1. Baker, R. W. Membrane Technology and Applications, 2nd ed.; Wiley: Chichester, 2004.
2. Ulbricht, M. Polymer 2006, 47, 2217.
3. Yoshikawa, M. Bioseparation 2002, 10, 277.
4. Ulbricht, M. J Chromatogr B 2004, 804, 113.
5. Wulff, G. Angew Chem Int Ed Engl 1995, 34, 1812.
6. Wulff, G. Chem Rev 2002, 102, 1.
7. Vlatkis, G.; Andersson, L. I.; Müller, R.; Mosbach, K. Nature 1993, 361, 645.
8. Haupt, K.; Mosbach, K. Chem Rev 2000, 100, 2495.
9. Katz, A.; Davis, M. E. Nature 2000, 403, 286.
10. Strikovsky, A. G.; Kasper, D.; Grun, M.; Green, B. S.; Hradil, J.; Wulff, G. J Am Chem Soc 2000, 122, 6295.
11. Ansell, R. J.; Mosbach, K. J Chromatogr A 1997, 787, 55.

12. Lai, J. P.; Lu, X. Y.; Lu, C. Y.; Ju, H. F.; He, X. W. Anal Chim Acta 2001, 442, 105.
13. Wang, J. F.; Cormack, P. A. G.; Sherrington, D. C.; Khoshdel, E. Angew Chem Int Ed Engl 2003, 42, 5336.
14. Boonpangrak, S.; Prachayasittikul, V.; Bulow, L.; Ye, L. J Appl Polym Sci 2006, 99, 1390.
15. Piletsky, S. A.; Dubei, I. Y.; Fedoryak, D. M.; Kukhar, V. P. Biopolym Kletka 1990, 6, 55.
16. Yoshikawa, M.; Izumi, J.; Kitao, T. Chem Lett 1996, 8, 611.
17. Kobayashi, T.; Wang, H. Y.; Fuji, N. Anal Chim Acta, 1998, 365, 81.
18. Wang, H. Y.; Kobayashi, T.; Fujii, N. J Chem Technol Biotechnol 1997, 70, 355.
19. Dzgoev, A.; Haupt, K. Chirality 1999, 11, 465.
20. Sergeyeva, T. A.; Piletsky, S. A.; Piletska, E. V.; Brovko, O. O.; Karabanova, L. V.; Sergeeva, L. M.; El'skaya, A. V.; Turner, A. P. F. Macromolecules 2003, 36, 7352.
21. Lehmann, M.; Brunner, H.; Tovar, G. E. M. Desalination 2002, 149, 315.
22. Silvestri, D.; Borrelli, C.; Giusti, P.; Cristallini, C.; Ciardelli, G. Anal Chim Acta 2005, 542, 3.
23. Kobayashi, T.; Wang, H. Y.; Fujii, N. Anal Chim Acta 1998, 365, 81.
24. Mathew-Krotz, J.; Shea, K. J. J Am Chem Soc 1996, 118, 8154.
25. Piletsky, S. A.; Matuschewski, H.; Schedler, U.; Wilpert, A.; Piletska, E. V.; Thiele, T. A.; Ulbricht, M. Macromolecules 2000, 33, 3092.
26. Kochkodan, V.; Weigel, W.; Ulbricht, M. Analyst 2001, 126, 803.
27. Hilal, N.; Kochkodan, V. J Membr Sci 2003, 213, 97.
28. Dhal, P. K.; Arnold, F. H. J Am Chem Soc 1991, 113, 7417.
29. Matsui, J.; Nicholls, I. A.; Takeuchi, T. Anal Chim Acta 1996, 335, 71.
30. Zheng, N.; Li, Y. Z.; Wang, Z. M.; Chang, W. B.; Li, T. J. Acta Chimi Sin 2001, 59, 1572.
31. Wu, L. Q.; Li, Y. Z. Anal Chim Acta 2003, 482, 175.
32. Kimaro, A.; Kelly, L. A.; Murray, G. M. Chem Commun 2001, 14, 1282.
33. Araki, K.; Maruyama, T.; Kamiya, N.; Goto, M. J Chromatogr B 2005, 818, 141.
34. Ma, X. X.; Li, W. Y.; He, X. W.; Zhang, Y. K. Acta Chimi Sin 2005, 63, 1681.
35. Khayet, M.; Feng, C. Y.; Khulbe, K. C.; Matsuura, T. Desalination 2002, 148, 321.
36. Yang, Z. G.; Xu, Z. L.; Chen, G. E.; Xie, Y. Z. J Chem Ind Eng (China) 2007, 58, 125.
37. Zhou, J.; He, X. W. Anal Chim Acta 1999, 381, 85.
38. Tunc, Y.; Hasirci, N.; Yesilada, A.; Ulubayram, K. Polymer 2006, 47, 6931.
39. Wang, X. J.; Xu, Z. L.; Yang, Z. G.; Bing, N. C. Prog Chem 2007, 19, 805.
40. Wang, X. J.; Xu, Z. L.; Bing, N. C.; Yang, Z. G. Chin J Chem Eng 2007, 15, 595.